

## Structure and magnetism of quasicrystalline and crystalline $\text{Al}_{1-x}\text{Mn}_x$ alloys

S. E. Youngquist, P. F. Miceli, D. G. Wiesler, and H. Zabel

*Department of Physics and Materials Research Laboratory, University of Illinois at Urbana-Champaign, Urbana, Illinois 61801*

H. L. Fraser

*Department of Metallurgy and Materials Research Laboratory, University of Illinois at Urbana-Champaign, Urbana, Illinois 61801*

(Received 10 March 1986)

We have performed x-ray structural studies of quenched and annealed  $\text{Al}_{1-x}\text{Mn}_x$  alloys in the range of  $0.14 \leq x \leq 0.20$ . The quenched samples exhibit a coexistence of Al with an icosahedral phase, the latter having a maximum volume fraction at  $x=0.20$ . Magnetic susceptibility measurements for  $x=0.14$  and 0.20 show a dramatically enhanced magnetic moment in the icosahedral phase ( $p=0.747$  and 1.27, respectively) as compared to the annealed samples ( $p=0$  and 0.617, respectively). The increase of magnetic moment per Mn ion with increasing Mn concentration indicates a range of stoichiometries and microstructures over which the icosahedral phase can exist.

Rapidly quenched  $\text{Al}_6\text{Mn}$  was recently reported to exhibit icosahedral symmetry, which is incompatible with conventional crystalline order.<sup>1,2</sup> This discovery prompted an upsurge of experimental and theoretical activity to understand the underlying structure and its effect on the physical properties of the material. It has been observed that quasiperiodic space-filling structures (three-dimensional Penrose tilings) can give rise to diffraction patterns in qualitative agreement with experiment.<sup>3,4</sup> However, discrepancies with regard to observed peak widths have produced speculation on the role of disorder in these solids.<sup>5-7</sup> Further experimental investigation into their structure and physical properties will help to illuminate these issues. To this purpose, we have studied in detail the compositional dependence of the magnetism and of the relative amount of icosahedral phase in  $\text{Al}_{1-x}\text{Mn}_x$  alloys.

Alloys of composition  $0.1 \leq x \leq 0.27$  were produced by melt spinning, using a 6-in. 1020 FeC-coated Cu wheel with a surface velocity of 35 m/sec. The ribbons had an average thickness of  $\sim 50 \mu\text{m}$ . The composition of each ingot was determined by weight to better than 0.5%. X-ray measurements were carried out in the energy dispersive mode using a Si(Li) detector. Preliminary x-ray studies showed that the most reliable and reproducible data are obtained from pulverized ribbons. Subsequent measurements were then carried out on  $\text{Al}_{1-x}\text{Mn}_x$  powder held in thin-walled Lindemann glass tubes.

Figures 1(a)–1(d) show x-ray scans of quenched Al-Mn alloys with increasing Mn concentration. In the first three spectra, an Al powder pattern coexists with reflections from the icosahedral phase. Icosahedral peak positions were checked against published values,<sup>3</sup> and are labeled in accordance with the theories of Elser.<sup>8</sup> As the Mn concentration is increased, the integrated intensity of the Al peaks decreases continuously relative to the icosahedral reflections.

In Fig. 2, the intensity ratio of the icosahedral (211111)

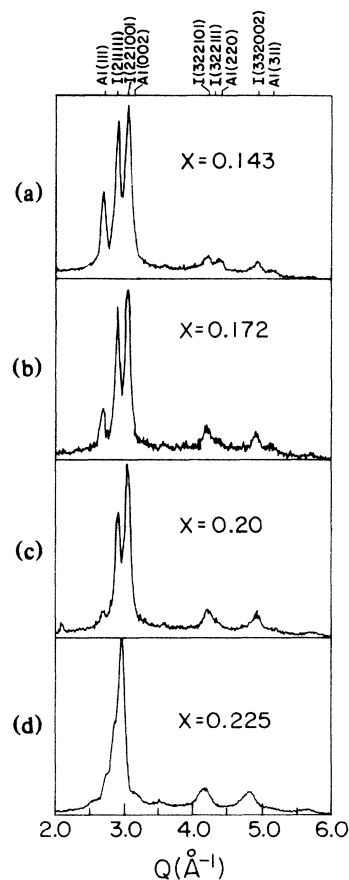


FIG. 1. (a)–(d): Energy dispersive x-ray scans of  $\text{Al}_{1-x}\text{Mn}_x$  alloys for various compositions  $x$ . The energy scale is converted to a scattering vector scale via  $Q = (2E/hc) \sin\theta$ , where  $\theta$  is the fixed scattering angle (here  $\theta=7.5^\circ$ ). In (a)–(c) the icosahedral peaks are indexed according to Elser's indexing scheme (Ref. 8). In (d) the reflections correspond to the  $T$  phase.

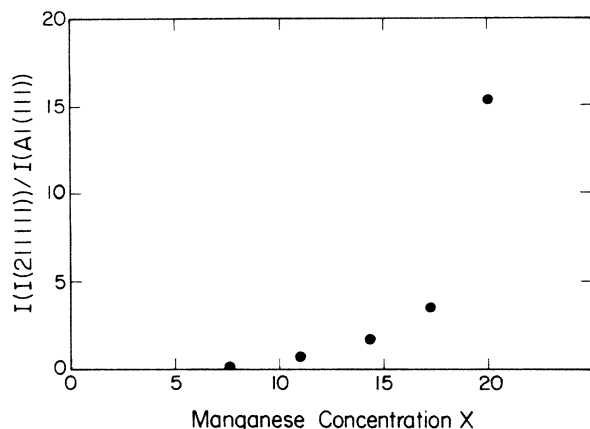


FIG. 2. The integrated intensity ratio of the Al(111) and the icosahedral (2111111) peaks are plotted as a function of the Mn composition. Beyond  $x=0.20$  the Al and icosahedral reflections disappear and are replaced by those of the  $T$  phase.

to the Al(111) peak is plotted as a function of the Mn concentration. From this plot we conclude that the maximum relative amount of icosahedral phase is obtained at a composition of  $x=0.20$ , corresponding to the stoichiometry  $\text{Al}_4\text{Mn}$ , rather than  $\text{Al}_6\text{Mn}$  as thought previously. At higher Mn concentrations [Fig. 1(d)], the diffraction pattern changes qualitatively, with new peaks occurring, indicating the new structure known as the  $T$  phase.<sup>9</sup> On the resolution scale of this experiment ( $\Delta Q/Q=0.01$ ) the icosahedral peak shapes remain the same until the Mn concentration reaches  $x=0.22$ . Higher-resolution angle-dispersive experiments on peak shape and position are in progress.

An important clue to the structural relationship between crystalline and quasicrystalline phases of Al-Mn can be derived from measurements of the magnetic susceptibility. We measured the dc magnetic susceptibility of both the quasicrystalline and annealed (crystalline) forms at two Mn concentrations:  $x=0.143$  and  $x=0.20$ , to be referred to as AN14, AN20 for the annealed, and QC14, QC20 for the quasicrystalline samples. These compositions correspond to  $\text{Al}_6\text{Mn}$  and  $\text{Al}_4\text{Mn}$ , respectively, whose crystalline structures are reported in the literature.<sup>10-12</sup>

Crystalline samples for the magnetic susceptibility studies were prepared by annealing of the quenched Al-Mn powder. The  $\text{Al}_6\text{Mn}$  powder was annealed first at  $390^\circ\text{C}$  for  $\sim 24$  h, then at  $500^\circ\text{C}$  for 6 h to ensure crystallization. The  $\text{Al}_4\text{Mn}$  sample was annealed at higher temperatures:  $700^\circ\text{C}$  for 24 h,  $750^\circ\text{C}$  for 12 h, and  $800^\circ\text{C}$  for 21 h. X-ray spectra were taken periodically during the annealing process to verify the change of phase. The measurements were performed with a superconducting quantum interference device (SQUID) magnetometer using a 10-kOe field and temperatures ranging from 1.7 to 300 K. Roughly 0.1 g of finely ground powder was contained in a thin Mylar bag. Although nearly negligible, the magnetization of the Mylar bag was measured independently and was subtracted from the total magnetization.

In Fig. 3 the magnetic susceptibility per mole of Mn is plotted as a function of temperature for all four samples.

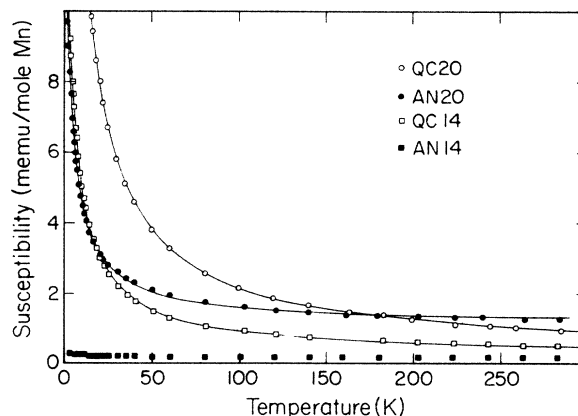


FIG. 3. Magnetic susceptibility as a function of temperature measured in a field of 10 kOe. QC14, QC20 designate quasicrystalline samples of  $\chi=0.143$  and  $0.20$  Mn concentration, respectively, AN14, AN20 designates samples of same composition but annealed.

The salient feature of this figure is the dramatic increase in the magnetic susceptibilities of both quasicrystalline phases as compared to their crystalline counterparts. In fact, crystalline  $\text{Al}_6\text{Mn}$  exhibits no Curie-Weiss-type paramagnetism at all. The solid lines are fits to the data points by a Curie-Weiss law plus a constant:  $\chi = (\mu_B^2 p^2 / 3k_B) / (T + \Theta) + \chi_0$ , where  $\mu_B$  is the Bohr magneton,  $k_B$  is the Boltzmann constant,  $\Theta$  is a negative Curie temperature, and  $p$  is the effective moment. The fit parameters are listed in Table I. The  $J$  values are calculated from  $p^2 = g^2 J(J+1)$ , assuming a spin-only Landé factor  $g=2$ .

Our experiments on AN14 and AN20 agree well with published data from Taylor,<sup>13</sup> who also reports that  $\text{Al}_6\text{Mn}$  is nonmagnetic. However, since his data extend only to 77 K, Taylor's reported values of  $p$  and  $\Theta$  for  $\text{Al}_4\text{Mn}$  are significantly in error.

The  $J$  values derived from our measurements show that a small portion of the total available  $d$  electrons participate in the magnetism since photoemission studies on Al-Mn alloys indicate that there are roughly 6  $d$  electrons for Mn (Ref. 14) at these compositions. Because the interaction of  $d$  electrons with the conduction electrons is known to depolarize the  $d$  states,<sup>15,16</sup> localization of some conduction electrons might explain an enhanced  $d$ -state polarization in the quasicrystalline phase. Such localization in quasiperiodic systems has been speculated theoretically.<sup>17-19</sup> However, it is unclear whether the enhanced magnetization would also be present in the amorphous phase,

TABLE I. Fit parameters for magnetic susceptibility measurements shown in Fig. 3.

Sample	$\Theta$ (K)	$\chi_0$ (memu/mol)	$p$ (units of $\mu_B$ )	$J$
QC20	5.92	0.32	1.27	0.307
AN20	3.76	1.48	0.617	0.087
QC14	4.77	0.23	0.747	0.124

or if it is a real consequence of quasiperiodicity. Another possible contribution to the larger  $J$  value for the quasicrystal may be manifested in the symmetry of the crystal field. Icosahedral symmetry is much closer to producing isotropic crystal fields than the orthorhombic and hexagonal crystal phases, and therefore the quenching of the orbital angular momentum may not be complete. Recent calculations<sup>18</sup> of the electronic properties of Al-Mn clusters also show that icosahedral symmetry introduces degeneracy in the energy levels. However, recent results of Mossbauer<sup>20</sup> and extended x-ray absorption fine-structure<sup>21</sup> measurements seem to indicate the existence of two types of Mn sites, each with some amount of asymmetry. These results seem to indicate an increased localization of the conduction electrons.

As our x-ray data demonstrate, the quasicrystalline phase exists over a range of Mn concentrations, and we might ask whether or not the quasicrystal is always the same entity. From the magnetic susceptibility we find that the quasicrystal  $J$  values differ by more than a factor of 2 for the two compositions  $x = 0.14$  and  $x = 0.20$ . More recent high-resolution x-ray data indicate<sup>22</sup> that the positions of the icosahedral reflections shift with the Mn concentration. Both results are strong evidence that the quasicrystalline structure and stoichiometry has a range of existence and may not be unique. Denoting the composition of the quasicrystalline phase itself by  $Al_{1-y}Mn_y$ ,  $y$  is calculated from the observed integrated intensities to vary by  $\Delta y \cong 0.056$  over the range of sample compositions studied, with a lower limit  $\Delta y > 0.035$ . Any Penrose tiling model would be required to accommodate this variation in

stoichiometry by variation of the decoration of the tiles. It is also interesting to note that crystalline  $Al_4Mn$  exhibits the largest magnetic moment of all the crystalline phases of Al-Mn alloys, most of which do not exhibit a Curie-Weiss behavior. This seems to indicate that crystalline  $Al_4Mn$  is more akin to the quasicrystalline structure than other compositions.

In conclusion, we have found from x-ray data a maximum volume fraction of icosahedral phase in  $Al_{1-x}Mn_x$  at the composition  $x = 0.20$ . Comparison of the magnetic susceptibility between quasicrystalline and annealed crystalline materials of  $x = 0.14$  and  $0.20$  showed that the quasicrystalline phase has consistently higher magnetic moment, again with a maximum moment for  $x = 0.20$ . We would like to note that after our original manuscript was submitted, Hauser, Chen, and Waszczak<sup>23</sup> published work on the magnetic susceptibility of the quasicrystalline phase. However, in contrast to their work, we have demonstrated that enhanced magnetic properties are a consequence of the quasicrystalline state. The combination of our x-ray and magnetic studies leads to the suggestion that the icosahedral phase exhibits a range of stoichiometry and microstructure.

We would like to thank D. A. Neumann for helpful discussions. One of us (S.E.Y.) gratefully acknowledges support from AT&T Bell Laboratories. This work was supported in part by the National Science Foundation under Grant No. DMR83-04890 and by the U.S. Department of Energy, Division of Materials Sciences, under Contract No. DE-AC02-76ER01198.

<sup>1</sup>D. Shechtman, I. Blech, D. Gratias, and J. W. Cahn, *Phys. Rev. Lett.* **53**, 1951 (1984).  
<sup>2</sup>R. D. Field and H. L. Fraser, *Mater. Sci. Eng.* **68**, L17 (1984).  
<sup>3</sup>P. A. Bancel, P. S. Heiney, P. W. Stephens, A. I. Goldman, and P. M. Horn, *Phys. Rev. Lett.* **54**, 2422 (1985).  
<sup>4</sup>D. Levine and P. J. Steinhardt, *Phys. Rev. Lett.* **53**, 2477 (1984).  
<sup>5</sup>P. W. Stephens and A. I. Goldman, *Phys. Rev. Lett.* **56**, 1168 (1986).  
<sup>6</sup>P. M. Horn (unpublished).  
<sup>7</sup>J. L. Robertson, M. E. Misenheimer, S. C. Moss, and L. Bendersky (unpublished).  
<sup>8</sup>V. Elser, *Phys. Rev. B* **32**, 4892 (1985).  
<sup>9</sup>R. J. Schaefer, L. A. Bendersky, D. Schechtman, W. J. Boettinger, and F. S. Biancanello (unpublished).  
<sup>10</sup>A. D. I. Nicol, *Acta Crystallogr.* **6**, 285 (1983).  
<sup>11</sup>A. Kontino and P. Coppens, *Acta Crystallogr. Sect. B* **37**, 433 (1981).

<sup>12</sup>M. A. Taylor, *Acta Metall.* **8**, 256 (1980).  
<sup>13</sup>M. A. Taylor, *Proc. Phys. Soc. London* **78**, 1244 (1961).  
<sup>14</sup>A. Wenger, G. Burri, and S. Steinemann, *Solid State Commun.* **9**, 1125 (1981).  
<sup>15</sup>P. W. Anderson, *Phys. Rev.* **124**, 41 (1961).  
<sup>16</sup>J. B. Dunlop, G. Gruner, and A. D. Caplin, *J. Phys. F* **4**, 2203 (1974).  
<sup>17</sup>T. Odagaki and D. Nguyen, *Phys. Rev. Lett.* **33**, 2184 (1986).  
<sup>18</sup>M. E. McHenry, M. E. Eberhart, R. C. O'Handley, and K. H. Johnson, *Phys. Rev. Lett.* **56**, 81 (1986).  
<sup>19</sup>F. Nori and J. P. Rodriguez, *Phys. Rev. B* **34**, 2207 (1986).  
<sup>20</sup>L. J. Swartzendruber, D. Shechtman, L. Bendersky, and J. W. Cahn, *Phys. Rev. B* **32**, 1382 (1985).  
<sup>21</sup>E. A. Stern, Y. Ma, and C. E. Bouldin, *Phys. Rev. Lett.* **55**, 2172 (1985).  
<sup>22</sup>S. E. Youngquist, P. F. Miceli, and H. Zabel (unpublished).  
<sup>23</sup>J. J. Hauser, H. S. Chen, and J. V. Waszczak, *Phys. Rev. B* **33**, 3577 (1986).